sustainability

MDPI

Article

Three-Dimensional Urban Air Networks for Future Urban Air Transport Systems

Chiara Caterina Ditta * and Maria Nadia Postorino *

Department of Civil, Chemical, Environmental and Materials Engineering, (DICAM)—Alma Mater Studiorum University of Bologna, 40126 Bologna, Italy

* Correspondence: chiaracaterina.ditt2@unibo.it (C.C.D.); marianadia.postorino@unibo.it (M.N.P.)

Abstract: Advances in new electric aerial vehicles have encouraged research on pioneering Urban Air Mobility (UAM) solutions, which would provide fast service for passengers, goods, and emergencies. From this perspective, some air service scenarios have been identified, such as air taxis, airport shuttles, and intercity services. Such air services should be supported by a suitable urban air network, which should comply with several boundary conditions linked to the specific features of this new type of aerial mobility. This paper proposes an Urban Air Network (UAN) model that includes a third (vertical) dimension and whose aim is to satisfy the basic principle of linking origin/destination pairs, as in usual ground transportation networks, by guaranteeing at the same time safe aerial paths between origin/destination pairs with suitable vehicle separations. The proposed UAN consists of multiple 2D graphs on different layers, which allows for the transfer of aerial vehicles in lower airspace. A suitable cost function has been associated with each UAN link in order to compute the shortest paths connecting the origin/destination pairs. The links in a UAN have a dynamic nature and can be enabled or disabled in consideration of capacity issues. In addition, indirect CO_2 emissions linked to aerial vehicles (such as operational and disposal phase charges) have been computed to foresee the potential environmental impacts based on the proposed UAN model. The preliminary results of a test case show encouraging results and provide interesting findings for further advancements.

Keywords: dynamic links; 3D model; flying vehicles; urban air mobility

Citation: Ditta, C.C.; Postorino, M.N. Three-Dimensional Urban Air Networks for Future Urban Air Transport Systems. *Sustainability* **2023**, *15*, 13551. https://doi.org/10.3390/su151813551

Academic Editors: Muhammad Zaly Shah, Eng. Muhammad Isran Ramli and Antonio Nelson Rodrigues da Silva

Received: 6 August 2023
Revised: 4 September 2023
Accepted: 6 September 2023
Published: 11 September 2023

1. Introduction

Recent advancements in aircraft technologies, electric propulsion, software, sensors, and communications have led to the development of unmanned aerial vehicles (UAVs), remotely piloted or fully autonomous, which were first implemented in specific geographic regions at a low risk level [1] for applications such as traffic monitoring [2], infrastructure inspection [3], mapping [4], and agriculture [5]. The ongoing UAV technological advancements [6] and the growing interest in their related systems (such as communications, sensors, and software) [7] have paved the way for a new concept of transportation systems in urban environments, which may take advantage of the vertical dimension for faster trips while maintaining high standard levels—so-called Urban Air Mobility (UAM). Specifically, Urban Air Mobility has been proposed as a safe, sustainable, and accessible urban transportation system for passengers and goods, as well as for emergency services in complex environments, such as metropolitan areas, by using both manned and unmanned vehicles to run on-demand and scheduled services [8]. It is assumed that in the beginning, the UAM system will be characterized by manned flying vehicles, afterward moving to fully autonomous vehicles with collision avoidance [9] and real-time route maintenance [10]. Many technical challenges, in terms of resource and power management, security, and communications, are involved in UAM development, together with issues related to air traffic management, noise, weather, environmental impacts, and regulations [11]. Furthermore,

an analysis of people's concerns about this new aerial mobility system carried out by the European Union Aviation Safety Agency (EASA) [12] has shown that safety and security are the main worrying aspects of UAM services, together with noise, environmental pollution, and privacy violations. Moreover, some studies have found that factors such as noise pollution and the amount of greenhouse gas emissions would have a key role in the successful adoption of UAM [13]. In comparison to usual ground transportation systems, this aerial transportation system includes a third spatial dimension and aerial services are expected to be realized mainly by some (still prototypal) electric Vertical Take-off and Landing (eVTOL) vehicles, which would have reduced environmental impacts compared to current low-altitude aerial vehicles (e.g., traditional helicopters). Although there have been many advancements towards making prototypal eVTOLs operational, there are still many issues to be solved in terms of both the virtual infrastructures that would support the implementation of aerial services in urban areas and the identification of their impacts.

The services provided by traditional ground transportation systems—such as transit services—and their performance are simulated by using the "transportation supply" model, which includes the technical and organizational aspects of the physical transportation supply in order to represent the topological and functional structure of the system [14]. The bases for many ground supply transportation models are network models, which combine graph models, defined by nodes and links, with the performance and cost functions associated with each network link [15]. Although there are still many aspects to be studied, from the features of aerial vehicles to safety and environmental concerns and scenario simulations [1,7,16,17],which are crucial for including the new "air mobility" in urban environments—such basic supply concepts apply to UAM scenarios as well. In this case, the technical and organizational aspects refer to an effective framework that will ensure safe operations and air vehicle separation and routes while avoiding interference with traditional aviation. Urban Air Network (UAN) models are intended to support flight services at low altitudes, mainly in the uncontrolled ICAO class G [18]. As for aerial services, a list of potential use cases has been drafted by NASA researchers [8]: air taxi on-demand service, air cargo, air metro, emergency operations, news gathering, and traffic and weather monitoring. As for passenger transport, several types of air services have now been defined in the literature with different characteristics and specific requirements for the UAM system [19–21]. Particularly, air taxis, airport shuttles, and intercity aerial services are expected to lead the international market in the coming decades (Figure 1).

Figure 1. Urban Air Mobility use cases.

UAN features supporting aerial services will depend on the nature of the implemented aerial service. An air taxi is similar to a ground taxi, i.e., an on-demand service for short-haul trips (expected distance from 15 to 50 km) [22]. An airport shuttle would provide scheduled flights between airports and strategic locations or points of interest (POI) in metropolitan areas for similar distance ranges as the air taxi service [23,24]. Finally, intercity scheduled services between cities would cover distances of more than 100 km and would allow direct access to POIs [25].

Combining the existing ground transportation networks with UANs could represent a great opportunity for urban and suburban mobility but would be a challenge for shaping the evolution of large metropolitan areas. In this multimodal transportation framework,

vertiports are the interchange nodes between aerial and ground services [26,27]. Such nodes, which are part of UAN models, are both take-off and landing sites for eVTOL, providing aerial services and passenger terminals for accessing/egressing the service. The location of vertiports should comply with several safety and security requirements and privacy issues, which would then affect the UAN structure.

A relevant difference between ground transportation networks and UAN is the vertical dimension of the latter, which is expected to provide advantages for overcoming ground congestion. Therefore, three-dimensional UANs should guarantee the following: (i) effective connections between POI in urban areas, (ii) reduced travel times and/or shorter travel distances, and (iii) effective and safe flight paths.

Another difference between ground and aerial urban network models is that UAN operability must be supported by data sharing and processing between eVTOL, or, more generally, Flying Vehicles (FVs), and ground air traffic control centres that could both avoid air traffic congestion, thanks to ad hoc communication networks, e.g., FANET [28] and WSNs [29,30], and provide safe separations among FVs [31]. These latter aspects are similar to what is expected, and partially operating in, Cooperative, Connected and Automated Mobility (CCAM) [32], which will use communication techniques such as V2V and V2I [33,34] to allow trips enabled by Connected and Automated Vehicles (CAVs).

Knowing data related to the status, positioning, and speed of each FV in UANs is one of the prerequisites for UAM operability, which also allows ground control centres to carry out management and regulatory operations for the maintenance of safety conditions. Particularly, two types of approaches have currently been specified to control and manage low–altitude urban air traffic: (1) centralized control system, such as Unmanned Aerial Systems (UASs) Traffic Management (UTM) or the U–Space Concept [35,36]; (2) route management directly realized using autonomous aerial vehicles with on-board technology, such as see–and–avoid supported by algorithms for route guidance [37].

In the above perspective, this paper proposes a three-dimensional Urban Air Network (3D-UAN) model that includes the third (vertical) dimension to link trip origin/destination points by sequences of aerial, dynamic links where a suitable cost function has been defined. The proposed UAN model has been applied for simulating some UAM services—particularly airport shuttles and intercity services—and for estimating indirect CO_2 emissions (such as those linked to operational, disposal phase charges) due to FVs moving on the 3D-UAN. Finally, such CO_2 emissions have been compared with those released by fuel engine cars under the same conditions.

The paper is organized as follows. Section 2 reviews the aerospace structure background for UAVs. Section 3 introduces the 3D network model, which could allow UAM operations in the near future, and describes both the specifications and implications of the model. Section 4 presents an experimental scenario and discusses network performances and results. Section 5 deals with the estimation of CO_2 in the experimental scenario, including the comparison of emissions for UAM services and fuel engine cars. Finally, in Section 6, some conclusions and future developments are drawn.

2. Literature Review

As set out in a previous review [38], a multi-layer graph model where links represent some kind of "airways" (corridors) and nodes allow transfers between layers has been proposed in the literature for uncontrolled (class G) aerospace [39]. In this model, FVs can move along such corridors and nodes without direct communication with a central control system (such as UTM); they are guided by both rules defined on the corridors themselves (speed limits, flight headings, and maximum traffic capacity) and information exchanged via V2V communications [33]. The geometrical features of the corridors depend on (1) the FV types that will occupy them (e.g., different sizes influence corridor cross-sections), (2) the distance between the Points of Interest (origin/destination nodes), and (3) the presence of fixed obstacles in the airspace.

However, the literature on UAN models that are designed explicitly for UAM services is rather poor. Most studies have focused on the characteristics and potential constraints of the lower airspace where FVs would move [40,41]. Although not directly addressed to model UANs for UAM services; nevertheless, these studies are useful to identify properly both features and properties by meeting the technical and operational requirements of such networks.

In order to allow safe operations and fast urban aerial services, some solutions have been proposed in the literature to plan the lower airspace environment. The Metropolis project [42] proposes four different urban concepts to study changing capacity: (i) Full Mix, (ii) Layer, (iii) Zone and (iv) Tube. Simulations carried out to validate these four concepts showed that a layered concept is optimal for urban air mobility services (e.g., personal air transport or delivery drones).

In detail, the Full Mix concept would be involved in free flight contexts—such as 'non–structured airspace'—where air traffic is subjected to physical constraints (e.g., weather, fixed obstacles), and FVs would autonomously handle separation and trajectory via on-board sensors and software [43]. In this context, the UAN model would simply identify a topological structure with links, i.e., aerial corridors, where flights are allowed and nodes at crossing points of such corridors and/or at vertiports.

The Layer concept includes an airspace designed in several layers, where separation among FVs is ensured by combining position, speed, and altitude settlement. This airspace structure is expected to reduce conflicts by limiting the relative speeds between FVs that cruise at the same altitude. Furthermore, the Layer concept meets the main features of a 3D–UAN, where different layers are identified, each one with its own horizontal structure and connections between layers that are ensured at specific points (nodes).

The Zone concept refers to circular and radial zones. Circular zones are used as ground roundabouts, while the radial zones connect and allow traffic to flow toward the circular zones.

Finally, the Tube concept provides a fixed structure with pre-planned, conflict-free routes, like a graph where nodes identify specific points and tubes (i.e., links) connect two nodes. In this structure, time separation between FVs is considered as the "fourth dimension"; when a FV passes a node, it "occupies" such node for a given interval, and during this time, no other FV can pass this node. This layout allows a multi-layer structure; particularly, operations in the lower levels are reserved for short-range flights, while the higher levels would be used for long-range flights.

Another concept for modelling lower airspace and identifying a UAN structure is offered by AirMatrix [44]. The AirMatrix network establishes an airspace structure divided into uniform air blocks arranged on multiple levels, which provides standardized units for urban airspace management. By assigning a different number of air blocks to each layer, the AirMatrix intends to manage the number of FVs that can move in the airspace by considering constraints like the number of waypoints, crossing points, and flight flexibility. Flight operations are managed by a trajectory-based approach, i.e., starting from pre-determined waypoints (origin and destination), FVs move between successive, intermediate waypoints to complete their path. This model assumes corridors where FVs are moving and might be considered a preliminary structure for providing UAM services. A simulation has been carried out to evaluate FV operation performance indicators such as average travelled distance and travel time. The results have shown that improvements are needed to handle an increasing number of FV operations.

In the Dynamic Delegated Corridors (DDCs) framework [45], airspace volumes or tunnels similar to airways are considered (Figure 2). The air traffic separation is entrusted to the autonomous decisions of FVs, which are supposed to be equipped with advanced tools ensuring see-and-avoid capabilities, navigation precision, and V2V connections. Corridor size and operating time may change and can be enabled (open/closed) according to weather conditions and air traffic density. DDCs are also supported by an Automated Decision

support service, and they might be seen as a dynamic UAN model, where links can be enabled or disabled according to some criteria.

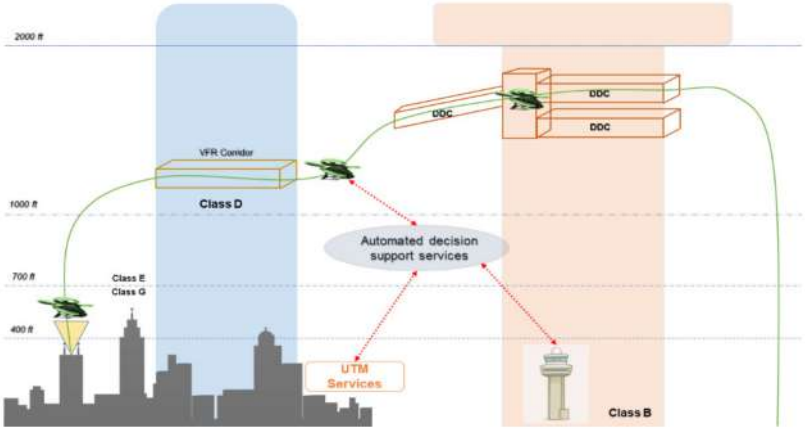

Figure 2. Dynamic Delegated Corridors (DDCs) airspace concept.

More recently, Wang et al. [46] introduced an air traffic planning methodology to ensure UAM operations by defining a fixed-route structure modelled as a graph, wherein volume segments act as links, supporting two-way traffic and vertiports (here named droneports) and delivery points act as nodes. Vertical links are added to connect the horizontal volume segments, and a cylindrical airspace volume is identified in which density points have been specified to measure the flow pattern constraints, which is designed to capture the complexity in each node. In addition, an objective function based on linear dynamic systems and specified as the sum of node complexities incorporates temporal and spatial information, such as link congestion and operational efficiency, to measure air traffic interaction. To minimize node complexity and optimize the UAM flow pattern in the proposed structure, a two-step algorithm (i.e., Simulated Annealing and Dafermos' metaheuristic algorithm) is explored by generating solutions to balance the path complexity in OD pairs and manage structure congestion.

Other studies, based on a free flight–aerospace approach, in which ground and low airspace constraints are identified by employing 3D GIS maps and evaluating strategic UAM paths by using collision-avoidance methods [47–49]. In [49], at first, the shortest path for each OD pair is computed using well-known shortest path algorithms (e.g., Dijkstra) in order to identify the flight collision configurations and their minimum temporal separation. Then, the route intersection information is employed for flight de-confliction and a pre-departure flight level assignment plus departure delay integration is proposed, to solve conflicts and specify suitable UAM paths. Another approach employs a digital twin model together with an aerial urban network model [50] to identify both relevant elements, such as ground access points and obstacle heights, by using dynamic data and optimal flight paths.

Starting from the above perspective, this paper proposes a three-dimensional Urban Air Network (3D-UAN) model, which complements and improves some preliminary studies present in the literature [39,45]. Particularly, the concept of dynamic corridors has been integrated with the multi-layer and corridor structure based on Layer concepts. In detail, the 3D-UAN model is composed of nodes corresponding to vertiports and/or singular points in the urban context and links connecting such nodes. Each layer is connected to the others by suitable vertical links. A link cost function has been defined to guarantee FV separations, avoid conflict points, and allow suitable traffic flow levels to ensure uncongested conditions and meet link capacity criteria. It is worthwhile to note that the network has been conceived to support flight operations based on the "see and avoid" concept [51], and each link is bi-directional. In other words, FVs can use one or the opposite link direction depending on (1) their origin/destination pair, and (2) the status of

the link, which might be enabled or disabled in the required direction based on the flight direction of another FV that is using the same link and/or the link spare capacity.

3. The Proposed 3D-UAN Model

A multi-layer three-dimensional network (3D–UAN) is here proposed (Figure 3) for supporting UAM services for passengers and freight in the very low and uncontrolled airspace, i.e., 500 ft above ground level [52]. The network includes ad hoc links, like DDCs, which are intended to be suitably enabled or disabled based on the information provided by data collected and transmitted by both connected FVs [43] and a centralized control system. As available data are thought to be both real-time and off-line (the latter being time series data), 3D-UAN operations will depend on both real-time and off-line data processing. FVs will share data on their position, speed, operating status, and environmental conditions with both other vehicles and the control centre by using V2V and V2I/V2X communication technologies [33,34].

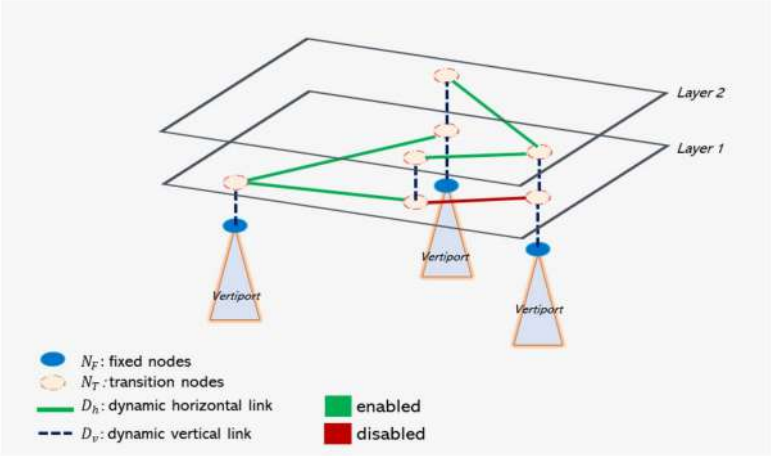

Figure 3. Three-dimensional Urban Aerial Network (3D-UAN) model.

Layers, nodes, links, and link cost functions are the relevant elements of the proposed 3D-UAN model for UAM operations. In detail, for each layer L, a two-dimensional graph G_L is defined, which includes the set of *fixed nodes* ($N_{F,L}$), the set of *transition nodes* ($N_{T,L}$) and the set of *dynamic links* (D_L).

Fixed nodes are identified in the access and egress points of the UAM network (i.e., locations having vertiport roles), while transition nodes correspond to positions where horizontal crossings and switches to an upper or lower layer are enabled. It is notable that some transition nodes have the same position as fixed nodes except for the vertical coordinate; for example, at vertiports, vertical switches may also occur.

Dynamic *links* (in the following also simply links) connect pairs of nodes—both fixed and transition. Each link $d_{m,L}$ represents the connection existing between two fixed nodes on the same layers or between a node—fixed or transition—in layer L and a node—fixed or transition—in another upper or lower layer. Dynamic links $d_{m,L}$ belong to the set $D_L = \{d_{m,L}\} \mid m = \{1, 2 \ldots K_L\}$, where K_L is the total number of links for layer L. They can be considered as air corridors that will be enabled or not based on traffic capacity and environmental conditions (e.g., accumulation of operational delays, adverse weather conditions). In addition, their geometrical features may change depending on the flight vehicle's characteristics and safe distance. Particularly, link length among two fixed nodes is related to FV energy consumption. In fact, the recharging facilities will be located at vertiports [53], and setting the maximum distance between them is crucial for ensuring safe flights. Furthermore, the size of each FV can affect link cross-sections by requiring an increase in the vertical separation for larger FVs (i.e., greater distance between the layers, vertical link length increase and changes in transition node positions) to guarantee suitable protection volumes around them [54].

Due to the 3D nature of the network model, the dynamic link set consists of horizontal and vertical link subsets, respectively:

$$D_{h,L} = \{h_{mL}\} \subset D_L \mid \mathrm{m} = \{1, 2 \ldots\}$$

$$D_{v,L} = \{v_{mL}\} \subset D_L \mid \mathrm{m} = \{1, 2 \ldots\}$$

Horizontal and vertical links only allow for some specific flight operations, i.e., landing and take-off operations, as well as layer transitions, which are permitted only on links belonging to the vertical link subset, while connections in the same layer occur only along links belonging to the horizontal link subset. Therefore, a given FV will move between layers by using vertical dynamic links, while horizontal dynamic links permit transfers within the same layer.

The final 3D Graph (Θ) includes the bi–dimensional graphs, G_L, and the subsets of vertical dynamic links $D_{v,L}$:

$$\Theta = \bigcup_{L=\{1,\ldots,n\}} G_L \cup D_{v,L}$$

with

$$G_L = (N_{F,L}, N_{T,L}, D_{h,L}) \tag{1}$$

By omitting the subscripts L and m for simplicity, the following link cost function $\boldsymbol{c}(T_t, T_g)$ has been associated with each link of Θ:

$$\boldsymbol{c}(T_t, T_g) = \begin{Bmatrix} T_{t_i} \text{ for } i = 1 \\ T_{t_i} + T_{g_{(i,i-1)}} \ \forall\, i > 1 \end{Bmatrix} \tag{2}$$

where i is the *i-th* FV using the dynamic link $d_{m,L}$ at a given time period; T_{t_i} is the travel time of i on the generic link; and $T_{g_{(i,i-1)}}$ is the time gap between i and *i–1*. In detail, the travel time T_{t_i} varies according to the link—horizontal vs. vertical. For horizontal links, T_{t_i} is the running time T_{r_i} if $i = 1$, which depends on FV features and possible air rules. If there is more than one FV on the same link, i.e., $i > 1$, the additional time $T_{g_{(i,i-1)}}$ ensures suitable separation between two subsequent FVs. This condition maintains safe travel conditions among FVs flying on the same path.

For vertical links, T_{t_i} may be climbing (T_{a_i}) or descend (T_{f_i}) time depending on the link direction—i.e., towards upper layers or towards lower layers. Again, the additional time $T_{g_{(i,i-1)}}$ ensures a suitable separation between two subsequent FVs also along vertical links.

Therefore, Equation (2) may be specified as follows:

$$c_{h,L}(T_r, T_g) = \begin{Bmatrix} T_{r_i} \text{ for } i = 1 \\ T_{r_i} + T_{g_{(i,i-1)}} \ \forall\, i > 1 \end{Bmatrix} \tag{3}$$

$$c_{v,L}\Big(T_a, T_f, T_g\Big) = \begin{cases} T_{a_i} \text{ for upper layer transitions, } i = 1 \\ T_{a_i} + T_{g_{(i,i-1)}} \text{ for upper layer transitions, } i > 1 \\ \\ T_{f_i} \text{ for lower layer transitions, } i = 1 \\ T_{f_i} + T_{g_{(i,i-1)}} \text{ for lower layer transitions, } i > 1 \end{cases} \tag{4}$$

It is worthwhile to note that the cost function, particularly the travel time component, is principally a random variable because of some external factors, such as weather conditions. However, in this first version of the UAN model, the cost function has been considered deterministic. In other words, times and network status correspond to ideal conditions where no external and/or internal disturbances exist so that the final status might be considered the best condition under some scheduled services.

Furthermore, to ensure controlled departures from fixed nodes $N_{F,L}$ and the effective flow distribution over the 3D-UAN, aerial vehicles have to comply with an assigned

headway time at each fixed node before starting the journey, which may be considered a waiting time component, as detailed in the headway function $\boldsymbol{h}(I_{N_F})$:

$$\boldsymbol{h}(I_{N_F}) = I_{N_{F_i}} + \sum_{j=1}^{n-i} I_{N_{F_{i-j}}} \quad (5)$$

where I_{N_F} is the headway time associated with each aerial vehicle before take-off and depends on the variables $T_{r_{i-1_{h_{mL}}}}$, $T_{a_{i_{v_{mL}}}}$ and $T_{g_{(i,\ i-1)d_{mL}}}$, specifically designed for each dynamic link:

$$\boldsymbol{I_{N_F}}\left(T_{a_{v_{mL}}}, T_{r_{v_{mL}}}, T_{g_{d_{mL}}}\right) = \begin{cases} T_{g_{(i,\ i-1)v_{mL}}} + \left[T_{r_{i-1_{h_{mL}}}} + \left(T_{g_{(i,\ i-1)h_{mL}}} + T_{a_{i_{v_{mL}}}}\right)\right] \text{ if } i-1 \text{ positioning ahead of destination node } N_{T,L} \\ T_{r_{i-1_{h_{mL}}}} + \left(T_{g_{(i,\ i-1)h_{mL}}} + T_{a_{i_{v_{mL}}}}\right) \text{ if } i-1 \text{ positioning over destination node } N_{T,L} \end{cases} \quad (6)$$

In (5) and (6), i is the *i–th* FV departing from the generic fixed node $N_{F,L}$ and flying to the generic transition node $N_{T,L}$; j refers to the FV ahead i, and n is the total number of FVs using the 3D-UAN at a given time. In detail, the *i-th* FV must wait at the fixed node $N_{F,L}$ a *headway time* $\boldsymbol{h}(I_{N_F})$ such that collisions—between it and other FVs crossing the network—do not occur at the next transition node, and separation time $T_{g_{(i,\ i-1)}}$ is constantly guaranteed in each link $d_{m,L}$. Finally, the generalized link cost function is obtained by combining both $\boldsymbol{h}(I_{N_F})$ and $\boldsymbol{c}(T_t,\ T_g)$, i.e., the node and dynamic link cost functions.

Once the cost functions have been defined, the minimum cost paths from the origin to destination points can be estimated, which depend on the number of FVs on those links in the given reference time (e.g., $i = 1$ or $i > 1$). The suitable paths meeting the minimum cost criteria may be computed by using iterative shortest path algorithms (e.g., Dijkstra, 1959 [55]) or A* [56], based on the identification of link sequences allowing the minimum travel cost. Among some criteria for identifying paths, FVs are allowed to switch layers in transition nodes only a limited number of times, depending on route length. The layer switch constraint is also useful in guaranteeing savings in battery autonomy and travel time. In fact, the layer switches involve greater energy consumption to perform hover operations, for which a reduced speed is also needed [57], which causes a consequent increase in the overall travel time.

As already introduced, the computation of the link cost is based on both offline and real-time data; the latter will made available due to V2V and V2I/V2X communication technologies. This double aspect allows applying the 3D-UAN model to both scheduled and unscheduled air services. For scheduled services (such as airport shuttle and intercity services), the shortest path is computed before FV departures. Thus, the network can be used in a "steady state" mode, and minimum paths are identified in advance depending on the expected points of conflict and number of flight operations, which allows for the detection of which links have to be enabled due to link capacity and safety issues [58].

For an on-demand service (such as AirTaxi), the network dynamic features are crucial. In this case, information on the occupancy status of the dynamic links has to be shared in real time. In this condition, both each FV and the control centre, which receive and share data with each other and among the other connected FVs, would compute the shortest path by processing such data. During the trip, if a dynamic link reaches its capacity limit, it will be "disabled" in order to maintain safety standards and avoid traffic jams and disruptions on the network. FVs will be distributed over the network by re-computing the shortest paths in the current conditions such that conflict-free trips are still guaranteed.

It is worthwhile to note that real-time data exchange and monitoring are crucial for scheduled services as well. In fact, if there is any kind of disruption on one or more links, the computation of the new path is similar to what occurs for unscheduled services, and the information will be provided in real time via a similar computation, i.e., based on the data received from the control centre and from the other connected FVs.

To summarize, the 3D–UAN model supports the simulation of the expected UAM scenarios described before (see Figure 1) by ensuring connections between origin/destination pairs at the minimum travel cost.

Finally, in this first version of the model, both the path and departing slot assignment for each FV follow a priority criterion that depends only on service scheduling. In particular, the take-off and landing priority criterion is marked and must be compatible with the time gap on the links and headway time at the fixed nodes, also guaranteed by the see-and-avoid approach related to communication techniques among FVs. In the event that an on-demand service integrates with a scheduled one, the scheduled flights will have priority, and the on-demand flight between two scheduled flights will be allowed if the time gap is sufficient.

4. Simulation Scenario: Results and Implications

In order to assess the proposed model and analyse the preliminary performance, a simulation scenario is described, focusing on the analysis of a scheduled UAM service—such as an airport shuttle or intercity service. In such scheduled services, flight plans and procedures are established before each departure, with the only variations being linked to unforeseen events such as adverse weather conditions, instrument disruptions, and emergency management. However, as introduced in the previous section, it has been assumed that ideal conditions occur without disturbances with respect to the scheduled plan in order to obtain a network status that can be considered ideal.

It is worthwhile to note that the application refers mainly to the aerial network; in other words, the access/egress times to fixed nodes, i.e., vertiports, and the time required for the "ground" operations to be carried out (e.g., embarkation, disembarkation, security checks) are neglected and only the air travel time on the 3D-UAN for some origin/destination pairs is considered. In fact, the total travel time for the entire journey also includes the ground leg component, which depends on vertiport locations and ground mode features. The computation of ground times is outside the scope of the study.

The network structure used to test the 3D-UAN model is depicted in Figure 4. Note that each link is bidirectional—for vertical links—the two directions are separated by suitable horizontal distances. The travel direction for a horizontal link will depend on its occupancy and safety conditions, i.e., no FVs running in opposite directions are allowed to use the same link at the same time.

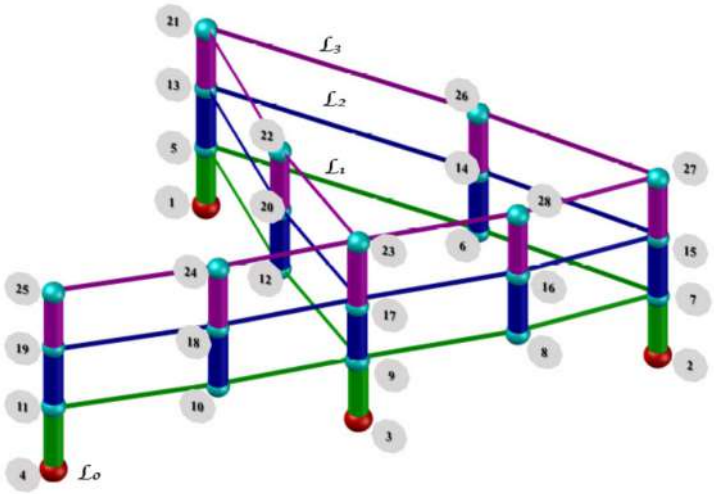

Figure 4. 3D-UAN structure used in the test case.

The test network includes four layers at 100 m from each other. At ground level ($\mathbf{L_0}$, 0 mt AGL), the air network accessibility occurs through four fixed nodes, corresponding to four vertiports. Each layer includes at least four transition nodes, which have the same position as the fixed nodes but different vertical coordinates. The remaining transition nodes have a different position—both horizontal and vertical coordinates—with respect to fixed nodes. Both fixed and transition nodes are connected via vertical dynamic links to the next layer (Figure 4). The main features of 3D–UAN, i.e., nodes and horizontal and vertical dynamic links, are shown in Table 1. In summary, the aerial network has four layers

(included the ground level), 28 nodes (including four vertiports), 40 vertical dynamic links, and 48 horizontal dynamic links (both directions).

Table 1. Nodes and dynamic link features in the 3D–UAN test case.

Vertical Links			Horizontal Links		
Dynamic Links *		Length (km)	Dynamic Links *		Length (km)
$\mathbf{L_0}$–$\mathbf{L_1}$	1–5	0.1	*Layer* $\mathbf{L_1}$	5–6	25.08
	2–7	0.1		6–7	31.05
	3–9	0.1		7–8	15.26
	4–11	0.1		8–9	20.81
$\mathbf{L_1}$–$\mathbf{L_2}$	5–13	0.1		9–10	18.03
	6–14	0.1		10–11	21.21
	7–15	0.1		9–12	17.69
	8–16	0.1		12–5	21.63
	9–17	0.1	*Layer* $\mathbf{L_2}$	13–14	25.08
	10–18	0.1		14–15	31.05
	11–19	0.1		15–16	15.26
	12–20	0.1		16–17	20.81
$\mathbf{L_2}$–$\mathbf{L_3}$	21–13	0.1		17–18	18.03
	22–20	0.1		18–19	21.21
	23–17	0.1		17–20	17.69
	24–18	0.1		20–13	21.63
	25–19	0.1	Layer $\mathbf{L_3}$	21–22	21.63
	26–14	0.1		22–23	17.69
	27–15	0.1		24–25	21.21
	28–16	0.1		23–24	18.03
				26–21	25.08
				26–27	31.05
				28–27	15.26
				28–23	20.81
Fixed Nodes	*Layer* $\mathbf{L_0}$				
	1, 2, 3, 4				
Transition Nodes	*Layer* $\mathbf{L_1}$		*Layer* $\mathbf{L_2}$		*Layer* $\mathbf{L_3}$
	5, 6, 7, 8, 9, 10, 11, 12		13, 14, 15, 16, 17, 18, 19, 20		21, 22, 23, 24, 25, 26, 27, 28

* Only links in one direction are reported for space reasons.

The simulation scenario considers the lift–cruise eVTOL prototype developed by Airbus (CityAirbus NextGen [59]) as a reference FV, which can reach 120 km/h (cruising speed) and has a range of 80 km. By considering the baseline scenario, a maximum capacity limit of two FVs in the same time interval has been assigned to each link, depending on the link lengths and the FV speed (Table 2). The average cruising speed allowed on the horizontal links is considered equal to 100 km/h, while on the vertical links (including take-off and landing phases), it is 45 km/h. This average speed value was chosen based on the CityAirbus NextGen data, which should also support issues related to flight safety.

Fourteen FVs have been considered operational during the simulation, travelling between six origin/destination pairs (Table 3). The simulation has been run for 70 min to explore the 3D-UAN model and, at the same time, allow all the involved FVs to reach their designated destinations. The simulation scenario started at time $t_0 = 0$, in which the first FV took off from vertiports 1, 2 and 4. To keep a safe time gap between the next two FVs flying the same link, the value of T_g has been set equal to 2 min. The headway time $\boldsymbol{h}(I_{N_F})$ has been ensured at fixed nodes before each departure. Particularly, FV_1, FV_2 and FV_3 take-off at time t_0 and their headway times I_{1_1}, I_{2_2} and I_{4_3} are equal to 0. Then, the minimum cost paths between OD pairs have been computed by a shortest cost path algorithm [55] based

on dynamic link requirements and constraints, i.e., links crossed in both directions and maximum capacity. By using Equations (2)–(6), time gap and headway time introduced above, the link costs have been calculated, and the minimum paths for each FV have been identified (Table 4).

Table 2. Dynamic link features in the baseline scenario.

Dynamic Link Characteristics	
Maximum link capacity (number of FVs)	2
Average cruise speed on horizontal links	100 km/h
Average cruise speed on vertical links	45 km/h

Table 3. FVs assigned to O-D pairs.

	Origin Node	Destination Node	Range
FV_1	1	2	56 km
FV_2	2	4	75 km
FV_3	4	2	75 km
FV_4	1	4	55 km
FV_5	1	3	39 km
FV_6	1	2	56 km
FV_7	2	1	56 km
FV_8	2	4	75 km
FV_9	2	4	75 km
FV_{10}	1	4	55 km
FV_{11}	1	3	39 km
FV_{12}	1	2	56 km
FV_{13}	1	4	55 km
FV_{14}	1	3	39 km

As previously stated, the simulation scenario refers to a scheduled service, and the air traffic flow is preliminarily estimated at each link before FVs take-off based on the available timetable. Consequently, some dynamic links have been enabled and disabled depending on capacity and collision avoidance issues.

As can be seen from Table 4, all the layers of the 3D-UAN are used to ensure optimal travel times and flight safety. In fact, flying vehicles FV_7, FV_8, FV_{10} and FV_{11} cross layer L_2 to reach their destination, while FV_{12}, FV_{13}, FV_{14} switch to layer L_3 because of both the capacity limits reached in lower layers and the requirement of T_g = 2 min on each link. Furthermore, at time t_Δ = 22 min from t_0, the link dynamic features are useful in managing FV flow on the aerial network. In fact, at node 9, FV_2 switches to L_2 to avoid collision with FV_3, which is flying in the opposite direction; consequently, link (9–10) is disabled while links (9–17) and (17–18) are enabled before FV_2 arrives. By considering the 3D-UAN at the time t_Δ= 22 min, the link occupation status and the distance travelled by the flying vehicles are reported in Table 5. These results allow both to evaluate whether the various dynamic links are enabled and disabled as expected and to identify potential conflict points on routes.

Table 4. Results of the 3D-UAN model for the simulation scenario.

OD Pair		Path	Link Cost *	Path Cost *	Travelled Distance *	OD Pair		Path	Link Cost *	Path Cost *	Travelled Distance *
1–2	**FV$_1$**	1–5 5–6 6–7 7–2	0.13 15.05 18.63 0.13	33.9	56.3	*2–4*	**FV$_2$**	2–7 7–8 8–9 9–17 17–18 18–19 19–11 11–4	0.13 9.16 12.49 0.13 10.82 12.73 0.13 0.13	45.7	75.7
	FV$_6$	1–5 5–6 6–7 7–2	6.53 15.05 18.63 0.13	40.3	56.3		**FV$_9$**	2–7 7–8 8–9 9–10 10–11 4–11	6.53 9.16 12.49 10.82 12.73 0.13	51.9	75.5
	FV$_{12}$	1–5 5–13 13–21 21–26 26–27 27–15 15–7 7–2	12.93 0.13 0.13 15.05 18.63 0.06 0.13 0.13	47.2	56.7		**FV$_{10}$**	2–7 7–15 15–16 16–17 17–18 18–19 19–11 11–4	8.67 0.13 9.16 12.49 10.82 12.73 0.13 0.13	54.3	75.7
4–2	**FV$_3$**	4–11 11–10 10–9 9–8 8–7 7–2	0.13 12.73 10.82 12.49 9.16 0.13	45.5	75.5						
2–1	**FV$_7$**	2–7 7–15 15–14 14–13 13–5 5–1	2.27 0.13 18.63 15.05 0.13 0.13	36.3	56.5	*1–4*	**FV$_4$**	1–5 5–12 12–9 9–10 10–11 11–4	2.27 12.98 10.62 10.82 12.73 0.13	49.5	78.8
1–3	**FV$_5$**	1–5 5–12 12–9 9–3	4.4 12.98 10.62 0.13	28.1	39.5		**FV$_8$**	1–5 5–13 13–20 20–17 17–18 18–19 19–11 11–4	4.4 0.13 12.98 10.62 10.82 12.73 0.13 0.13	51.9	79.0
	FV$_{11}$	1–5 5–13 13–20 20–17 17–9 9–3	10.8 0.13 12.98 10.62 0.13 0.13	34.8	39.7		**FV$_{13}$**	1–5 5–13 13–21 21–22 22–23 23–24 24–25 25–19 19–11 11–4	15.07 0.13 0.13 12.98 10.62 10.82 12.73 0.13 0.13 0.13	2.9	79.2
	FV$_{14}$	1–5 5–13 13–21 21–22 22–23 23–17 17–9 9–3	17.2 0.13 0.13 12.98 10.62 0.13 0.13 0.13	41.5	39.9						

* Distances are in km; costs are in minutes.

From the obtained results, it is revealed that setting three layers for fourteen FVs operating a 70 min service generally allows acceptable network operations. All the network layers had to be used, which increased the total time spent due to several climb/descend manoeuvres. The performance analysis of the FVs reported in Figure 5 shows interesting

and satisfactory results in terms of total travel costs and travelled distances, although introducing bidirectional links could lead to network overuse.

Table 5. Dynamic links status and FVs position at t_Δ = 22 min.

t_Δ = 22 min		Occupied Link	Travelled Distance *
1–2	**FV_1**	6–7	36.54
	FV_6	6–7	25.88
	FV_{12}	21–26	14.97
4–2	**FV_3**	10–9	36.54
2–4	**FV_2**	17–18	36.42
	FV_9	8–9	25.88
	FV_{10}	16–17	22.20
2–1	**FV_7**	14–13	32.87
1–3	**FV_5**	12–9	29.43
	FV_{11}	13–20	18.64
	FV_{14}	21–22	7.86
1–4	**FV_4**	12–9	32.99
	FV_8	20–17	29.31
	FV_{13}	21–22	11.41

* Distances are in km.

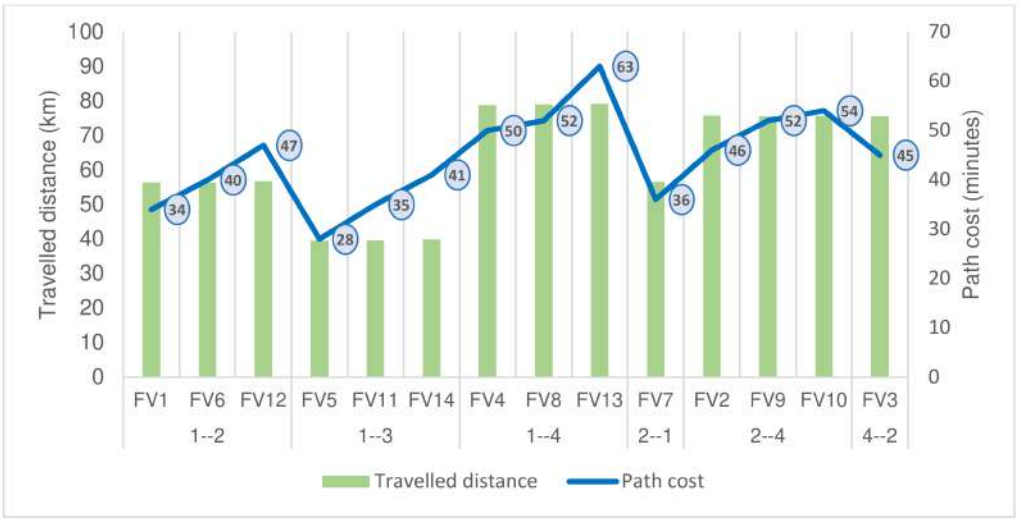

Figure 5. FV performances on the tested 3D-UAN per each OD pair.

Constraining the dynamic links to a capacity value of two flying vehicles in the same time interval guarantees a suitable safety level while maintaining service quality. Then, the hypothesized value T_g = 2 min is suitable to avoid conflict points and disruptions along the routes by keeping suitable separations between FVs, and it might be considered an optimal time gap for this test.

The analysed simulation scenario shows that the proposed cost function produces reasonable results. Running time mainly influences FV flows on network links, while the time gap and the consequent headway time may produce waiting times that can occur only at fixed nodes. Furthermore, the opportunity to move between layers depending on traffic needs allows optimal flow assignment and, at the same time, maintain safety standards. Opposed to ground transportation systems, there are no critical points, such as traffic light intersections, where significant, additional waiting time can affect the total path costs. Finally, the use of the dynamic link properties, i.e., enabled or disabled, depends on the identification (in real time) of the shortest paths between origin/destination pairs.

To apply the proposed 3D-UAN model to on-demand services (such as air taxis), ad hoc communication networks (FANET, WSN) [60] and continuous data exchange (e.g., FV positions, cruise speed, link status) between the individual FVs and the air traffic control centre are required in order to compute real-time shortest paths. However, the 3D-UAN model is the same as applied in the simulation scenario above. As an example, the event highlighted at time t_{Δ} = 22 min, i.e., link (17–18) enabled to ensure FV_2 transit, can be associated with an on-demand simulation since enabling and disabling links dynamically depending on traffic conditions appear to be satisfactory for this type of service. FVs may coordinate between themselves autonomously through the FANET system [28].

Through comparison with other studies reported in the literature, the proposed 3D-UAN model has a more comprehensive architecture as it proposes a well-defined network structure, which, in principle, includes the support of communicating networks and the link and node cost functions (2) and (5), computing the performance of the aerial network also from the user's perspective.

The 3D-UAN model has some innovative aspects with respect to the airspace models proposed in the current literature relating to UAM services (Table 6). At a first comparison based on Table 6, most of the existing models have a fixed Airspace Structure, which could generate some restrictions, particularly when introducing on-demand services. On the contrary, in the 3D-UAN model, the integration of dynamically activated corridors/airways, combined with the opportunity to move on different flight levels by entirely exploiting the third dimension, overcome the potential limitations of previous models in the literature. In detail, the 3D-UAN model combines the characteristics of a structured and controllable airspace using many layers at suitable altitudes for complying with aviation safety standards with the free flight flexibility by considering transitions nodes and dynamic links, which can be adapted in real time when needed.

Table 6. Existing lower airspace models vs. the proposed 3D-UAN model.

Models	Airspace Structure	Air Traffic Management
AirMatrix network [44]	Uniform air blocks arranged on multiple levels.	Pre-determined trajectory-based approach where FVs follow a set of waypoints assigned through conflict point detection
Dynamic Delegated Corridors [45]	Airspace volume or tunnels like airways.	Air traffic separation is entrusted to FV decisions (see-and-avoid) and supported by an automated decision support service on ground
Multi-layer Model [39]	Obstacle-free points in the different layers including corridors/airways.	Pre-determined path planning by minimising travel time and energy separately
Cylindrical volume with fixed-route structure [46]	Air network modelled as a graph, with volume segments as links and droneports as nodes.	Path planned through objective function specified as the sum of node complexities incorporates temporal and spatial information
Aerospace free flight approach [49]	3D GIS map provides obstacle-free airspace involving several layers.	Pre-departure flight level assignment involving collision—avoidance method
Proposed 3D—UAN	Multi-layer structure including dynamic links, fixed nodes (vertiports) and transition nodes	Shortest path calculated through ad hoc cost function including travel time, gap time among FVs on links and waiting time at vertiport and information

As for air traffic management, two main approaches may be identified from Table 6: (1) those based on the collision avoidance principle and communication between FVs to compute the air routes, and (2) those that, starting from an objective function, evaluate the complexities at the node and along the links to obtain the optimum paths. The proposed 3D-UAN model combines the above two approaches for air traffic management. In fact, the proposed cost function guarantees the minimum travel times and the separation standards between FVs by using information about air traffic on the network, which is collected through V2V and V2I technologies. Differently from the existing models that focus on one of the two methods, this framework exploits both the criterion of collision avoidance, which might also be used to simulate the network status in case of unforeseen events, and a structured objective function that satisfies the transport system principles by ensuring the shortest path computation between O/D pairs.

Finally, although the 3D-UAN framework can also be used for optimizing the fleet and services, in this study, the focus has been on the model feasibility for supporting UAM services. In other words, in this preliminary experiment, the 3D-UAN model has not been used for optimizing the network but for simulating the network status under some known conditions, e.g., scheduled services and/or on-demand services. Therefore, disturbances and potential disruptions are not the focus of this paper but future research.

5. A Preliminary Analysis of CO_2 Emissions and Comparison with Ground Vehicles

As introduced in Section 1, eVTOLs have been the key drivers for starting the concept of UAM services. Such flying vehicles do not produce CO_2 emissions directly during operations; in fact, eVTOLs are equipped with Distributed Electric Propulsion (DEP) engines [61]. However, operational and disposal phases may release CO_2 gas into the atmosphere [62]. Particularly, to be operational, FVs have to be recharged, and then they might contribute indirectly to CO_2 emissions based on how the electricity needed to recharge them has been produced.

In order to preliminarily explore the environmental impacts of UAM services in the framework of the proposed 3D-UAN model, an analysis of the indirect $kgCO_2$ produced in the simulation scenario tested in Section 4 has been performed. Such emissions have been compared to fuel engine car emissions in the same context, i.e., the same travelled distances under comparable traffic flow conditions. Particularly, the comparison has been referred to the Italian situation by considering some emission indexes estimated by ISPRA (Italian Institute for Environmental Protection and Research) [63]. The emission index (EI_{el}) in the power sector for electricity and heat production has been used, which only comes from fossil sources [63]. Such an index has been used for UAM trip CO_2 emissions, from the generation to the consumption of electricity needed to allow FV operations (Table 7). As for cars, the average emission factor for the car fleets circulating in Italy (EI_{car}) has been selected by the ISPRA national database [64], which is updated consistently with the COPERT version 5.5.1 ("COPERT is the EU standard vehicle emissions calculator, which uses vehicle population, mileage, speed and other data such as ambient temperature and calculates emissions and energy consumption for a specific country or region [65]) estimation model (Table 7). The EI_{car} factor is related to car fleets powered by petrol, diesel, LPG (Liquefied Petroleum Gas) and CNG (Compressed Natural Gas) fuels.

Table 7. Emission index for electricity production and passenger car estimated by ISPRA.

EI_{el} (gCO_2/kWh)	EI_{car} (gCO_2/km)
452.1	162.84

In this analysis, the power required by each FV in the simulation scenario described in Section 5 has been estimated by applying the approach proposed by Mudumba et al. [66],

which proposes uses Equations (7)–(10) to estimate the power required at different flight phases: hover, climb, cruise, and descent:

$$P_{hover} = \frac{mg}{\eta_h}\sqrt{\frac{\delta}{2\rho}} \tag{7}$$

$$P_{cruise} = \frac{mg}{\eta_c}\frac{V_{cruise}}{\frac{L}{D}} \tag{8}$$

$$P_{climb} = \frac{mg}{\eta_c}\left(ROC + \frac{V_{climb}}{\frac{L}{D}}\right) \tag{9}$$

$$P_{descent} = \frac{mg}{\eta_c}\left(ROD + \frac{V_{descent}}{\frac{L}{D}}\right) \tag{10}$$

where m is the total FV mass; g is gravity acceleration; L/D is the lift-to-drag ratio; η_h is the hover system efficiency; η_c is the climb and cruise system efficiency; ρ is the air density at sea level; ROD and ROC are Rate of Descent and Rate of Climb, respectively; V_{cruise}, V_{climb} and $V_{descent}$ are speeds adopted in different flight phases: cruise, climbing and descent.

Here, FV characteristics (Table 8) are based on available information from CityAirbus NextGen [59], while lacking data have been assumed by considering the features of a generic lift–cruise eVTOL prototype [62,67]. Finally, climb, cruise, and descent average speeds are the ones used for the simulation scenario (see Section 4).

Table 8. FVs (eVTOLs) main characteristics.

Reference	Variable	Value
CityAirbus NextGen—Airbus [59]	FV total mass m (kg)	2200
André and Hajek [62]	Disk loading δ (N/m^2)	627.5
André and Hajek [62]	L/D	8
Kasliwal et al. [67]	ROC (m/s)	5
Kasliwal et al. [67]	ROD (m/s)	–5
International standard Atmosphere [68]	ρ (kg/m^3)	1.225
André and Hajek [62]	η_c	0.63
André and Hajek [62]	η_h	0.765

CO_2 indirect emissions for the UAM tested service have been computed by employing the following equation [66]:

$$CO_{2(UAM)} = EI_{el}\left(\sum_{k \in flight\ phase} P_k \cdot t_k\right) \tag{11}$$

where P_k is the power required by each FV in a different flight phase and t_k is the travel time in a distinct flight segment (i.e., estimated link costs, see Table 4).

As for fuel engine car trips, CO_2 emissions have been computed by using the emission index EI_{car} and the travelled ranges between O/D pairs, which have been assumed to be the same as in the tested scenarios (see Table 3).

Emissions have also been computed per passenger. It has been assumed that FVs can accommodate the pilot and two passengers, and the indirect gas emissions have been evaluated for 42 people. For car trips, 21 passengers have been considered by adopting an average car occupancy rate of 1.6 [69], while the number of cars on the ground transportation network has been assumed to be the same as in the 3D-UAN scenario (14 vehicles).

The total kgCO_2 has been computed for both FV and car trips and *per* passenger travelling between the same O/D pair by FVs on the 3D-UAN and cars on the ground. The results are reported in Table 9.

Table 9. FV and car emissions $kgCO_2$ based on the simulation scenario.

Indirect CO_2 FV trip emissions	**CO_2 car trip emissions**
393.52 $kgCO_2$	131.25 $kgCO_2$
Indirect CO_2 emissions per passenger	**CO_2 emissions per passenger**
8.19 $kgCO_2$	5.86 $kgCO_2$

In the considered scenario and context—the travelled distances between O/D pairs being the same—the results show that FV operations produce more CO_2 gases than car trips, also in terms of emissions per passenger. This is an interesting preliminary result that must be further investigated. Although some studies [23,70] and some market analyses [71] propose UAM as a reduced carbon emission alternative to "traditional" mobility, there are some other studies that show less optimistic expectations with respect to the environmental impacts generated by UAM services [72]. This preliminary analysis is rather in line with this latter study, although it refers to a specific electricity generation case and cannot be generalized to other contexts. It should be noted that currently, eVTOL prototypes—such as Volocopter and Joby—have been investigated in terms of their main technical properties and characteristics, but the operational features of the different flight phases required for providing a real service like the tested one have not been completely explored yet. This is another source of uncertainty for the obtained results because some data had to be assumed based on other studies and hypotheses, which represents a probable limitation. In any case, although many aspects and elements require further in-depth investigations, these results show that using e-vehicles does not automatically correspond to a lower environmental impact, and attention must be paid to the way the electricity is generated, which applies to both aerial and terrestrial e-vehicles.

6. Conclusions

From the perspective of future UAM scenarios, this paper proposes an urban air network that explicitly uses the third dimension and supports the realization of air traffic in low airspace. Particularly, similarly to ground transportation system supply, this network model intends to characterize the urban aerial service supply for UAM systems by setting both the main topological features (i.e., a three-dimensional graph) and the link cost functions that shape the traffic flow on the transportation network.

The proposed multi-layer network model (3D-UAN) incorporates the concept of dynamic corridors, which are identified in the network links (both horizontal and vertical) and can be enabled or disabled according to link spare capacity and safety issues. As also emerged in the airspace literature, layer frameworks represent the airspace as a set of two-dimensional planes, which are connected via vertical corridors. In the context of urban aerial transportation systems, this layer-based space structure has been organized into an aerial transportation network composed of nodes and links with specific characteristics, also defined by the link cost functions that make it possible to compute the shortest paths based on the minimum travel cost criterion. Other than link travel time on both horizontal and vertical links, a suitable time gap on links and the headway time at fixed nodes have been assumed between the next FVs departures to guarantee suitable separations between FVs and avoid collision points on routes. To the best of these authors' knowledge, this work is the first that integrates the dynamism of air corridors by also associating a cost function in a multi-layer structure.

A simulation scenario has been generated to assess the network model and its feasibility. The results have shown the effectiveness and reliability of the proposed 3D-UAN model. A scheduled UAM transport service (as an airport shuttle) has been tested, in which origin and destination points are preliminarily established. Fourteen FVs have been assigned to the 3D network by using a shortest path algorithm combined with the specification of singular dynamic links to explore the performances of the adopted supply model. The obtained results confirm the suitability of the initial hypotheses (two FVs per link and a 2 min time gap between them) and show that the 3D-UAN model provides appropriate

outcomes in terms of path costs in relation to the travelled distances even if all the layers are occupied. It also emerged that using bi-directional dynamic links on the same layer could lead to network overuse.

In the test scenarios, some constraints have been set—such as a reduced average cruising speed value and a low value of the maximum capacity—which have to be further investigated in order to understand the effective limits of a UAM transportation system. Similarly, to test the potentialities of the supply model, some elements have to be further explored, such as higher speeds, a greater number of FVs, and longer travel ranges.

Finally, a preliminary analysis of the indirect CO_2 emissions produced when a scheduled aerial service is provided within the proposed 3D-UAN framework has been carried out. In detail, the $kgCO_2$ produced by FVs (indirect emissions linked to the electricity generation for the recharging phase) and cars (fuel engine direct emissions) in the tested scenario have been compared—all transportation features being the same and the necessary emission indexes referring to the Italian context. The results show that the tested UAM service generates higher levels of CO_2 than car trips per passenger travelling the same distances, which does not guarantee an effective advantage in proposing the UAM model as a sustainable alternative to traditional transportation systems in terms of greenhouse emissions. However, such results depend on the way the electricity is generated in the considered context, which could lead to completely different results in other contexts. Whatever the context, careful attention must be paid to the important aspect of how e-vehicles are charged, or, in other words, which is the source for generating electricity.

To summarize, the 3D-UAN model has shown interesting opportunities for modelling aerial transportation services in a multi-layer, 3D framework, and further developments are expected starting from this preliminary model. As for the link cost function, in this paper, it has been considered deterministic, but some factors could affect the time component—such as the weather conditions—so randomness should be explicitly considered. Weather conditions might affect energy consumption too, which in turn will impact travel times, and potential constraints in both link lengths and vertiport positioning should be included to ensure safety conditions. In addition, the 3D-UAN model has been used to simulate the network status under some known scheduled services. However, it may also be used to optimize the network, the criterion being times, fleet constraints, or some others. Another line of research will explore the introduction of "holding points" closed to vertical links to/from fixed points and the resulting additional waiting times. As for the network structure, further studies are expected for analysing the performances of a 3D-UAN model where the link directions are fixed for each layer, and directions change in alternate layers. Finally, the 3D-UAN model may be integrated into the overall urban supply transportation model by merging both the aerial 3D network and the ground transportation network and locating the fixed nodes (i.e., vertiports) in suitable POI in the ground network, such as airports, main railway stations, and city centres, by means of appropriate methods such as the GIS approach [73,74], the K-Means algorithm [75] and the Hub-location problem approach [76,77]. Thus, combining the 3D and ground networks will enable simulating an overall multi-mode ground–aerial transportation system.

Author Contributions: Conceptualization, C.C.D.; Methodology, C.C.D. and M.N.P.; Investigation, C.C.D.; Resources, C.C.D. and M.N.P.; Writing—original draft, C.C.D.; Writing—review and editing. C.C.D. and M.N.P.; Supervision, M.N.P.; Validation, M.N.P. All authors have read and agreed to the published version of the manuscript.

Funding: This research received no external funding.

Institutional Review Board Statement: Not applicable.

Informed Consent Statement: Not applicable.

Data Availability Statement: Not applicable.

Conflicts of Interest: The authors declare that they have no known competing financial interests or personal relationships that could have appeared to influence the work reported in this paper.

References

1. Bauranov, A.; Rakas, J. Designing airspace for urban air mobility: A review of concepts and approaches. *Prog. Aerosp. Sci.* **2021**, *125*, 100726. [CrossRef]
2. Sutheerakul, C.; Kronprasert, N.; Kaewmoracharoen, M.; Pichayapan, P. Application of unmanned aerial vehicles to pedestrian traffic monitoring and management for shopping streets. *Transp. Res. Procedia* **2017**, *25*, 1717–1734. [CrossRef]
3. Besada, J.A.; Bergesio, L.; Campaña, I.; Vaquero-Melchor, D.; López-Araquistain, J.; Bernardos, A.M.; Casar, J.R. Drone mission definition and implementation for automated infrastructure inspection using airborne sensors. *Sensors* **2018**, *18*, 1170. [CrossRef] [PubMed]
4. Hassanalian, M.; Abdelkefi, A. Classifications, applications, and design challenges of drones: A review. *Prog. Aerosp. Sci.* **2017**, *91*, 99–131. [CrossRef]
5. Grenzdörffer, G.J.; Engel, A.; Teichert, B. The photogrammetric potential of low-cost UAVs in forestry and agriculture. The International Archives of the Photogrammetry. *Remote Sens. Spat. Inf. Sci.* **2008**, *31*, 1207–1214.
6. Fan, B.; Li, Y.; Zhang, R.; Fu, Q. Review on the technological development and application of UAV systems. *Chin. J. Electron.* **2020**, *29*, 199–207. [CrossRef]
7. Cohen, A.P.; Shaheen, S.A.; Farrar, E.M. Urban air mobility: History, ecosystem, market potential, and challenges. *IEEE Trans. Intell. Transp. Syst.* **2021**, *22*, 6074–6087. [CrossRef]
8. Thipphavong, D.P.; Apaza, R.; Barmore, B.; Battiste, V.; Burian, B.; Dao, Q.; Feary, M.; Go, S.; Goodrich, K.H.; Homola, J.; et al. Urban air mobility airspace integration concepts and considerations. In Proceedings of the 2018 Aviation Technology, Integration, and Operations Conference, Atlanta, Georgia, 25–29 June 2018; p. 3676.
9. Jenie, Y.I.; Kampen, E.J.V.; Remes, B. Cooperative autonomous collision avoidance system for unmanned aerial vehicle. In *Advances in Aerospace Guidance, Navigation and Control*; Springer: Berlin/Heidelberg, Germany, 2013; pp. 387–405.
10. Sengupta, D.; Das, S.K. Urban Air Mobility: Vision, Challenges and Opportunities. In Proceedings of the 2023 IEEE 24th International Conference on High Performance Switching and Routing (HPSR), Albuquerque, NM, USA, 5–7 June 2023; pp. 1–6.
11. Idries, A.; Mohamed, N.; Jawhar, I.; Mohamed, F.; Al-Jaroodi, J. Challenges of developing UAV applications: A project management view. In Proceedings of the 2015 International Conference on Industrial Engineering and Operations Management (IEOM), Dubai, United Arab Emirates, 3–5 March 2015; pp. 1–10.
12. EASA. Study on the Societal Acceptance of Urban Air Mobility in Europe. 2021. Available online: https://www.easa.europa.eu/downloads/127760/en (accessed on 1 October 2022).
13. Liberacki, A.; Trincone, B.; Duca, G.; Aldieri, L.; Vinci, C.P.; Carlucci, F. The Environmental Life Cycle Costs (ELCC) of Urban Air Mobility (UAM) as an input for sustainable urban mobility. *J. Clean. Prod.* **2023**, *389*, 136009. [CrossRef]
14. Cascetta, E. *Transportation Systems Engineering: Theory and Methods*; Springer Optimization and Its Applications; Springer: New York, NY, USA, 2001; Volume 29.
15. Magnanti, T.L.; Golden, B.L. *Transportation Planning: Network Models and Their Implementation*; No. TR-143 Tech Rpt.; Massachusetts Institute of Technology, Operations Research Center: Cambridge, MA, USA, 1978.
16. Brown, A.; Harris, W.L. Vehicle design and optimization model for urban air mobility. *J. Aircr.* **2020**, *57*, 1003–1013. [CrossRef]
17. Postorino, M.N.; Sarné, G.M.L. Reinventing Mobility Paradigms: Flying Car Scenarios and Challenges for Urban Mobility. *Sustainability* **2020**, *12*, 3581. [CrossRef]
18. International Civil Aviation Organization (ICAO). *Annex 11: Air Traffic Secvices*; ICAO: Montreal, QC, Canada, 2001.
19. Baur, S.; Schickram, S.; Homulenko, A.; Martinez, N.; Dyskin, A. *Urban Air Mobility: The Rise of a New Mode of Transportation*; Roland Berger GmbH: Munich, Germany, 2018.
20. Schuchardt, B.I.; Becker, D.; Becker, R.G.; End, A.; Gerz, T.; Meller, F.; Metz, I.C.; Niklaß, M.; Pak, H.; Schier-Morgenthal, S.; et al. Urban Air Mobility Research at the DLR German Aerospace Center-Getting the HorizonUAM Project Started. In Proceedings of the AIAA Aviation 2021 Forum, Virtual Event, 2–6 August 2021; p. 3197.
21. Crown Consulting Inc.; Ascension Global; Georgia Tech Aerospace Systems Design Laboratory; McKinsey & Company. *Urban Air Mobility (UAM) Market Study*; Tech. Rep.; NASA: Washington, DC, USA, 2018.
22. Polaczyk, N.; Trombino, E.; Wei, P.; Mitici, M. A review of current technology and research in urban on-demand air mobility applications. In Proceedings of the 8th Biennial Autonomous VTOL Technical Meeting and 6th Annual Electric VTOL Symposium, Mesa, AZ, USA, 28 January–1 February 2019; pp. 333–343.
23. Cohen, A.; Shaheen, S. Urban Air Mobility: Opportunities and Obstacles. In *International Encyclopedia of Transportation*; UC Berkeley, Transportation Sustainability Research Center: Berkeley, CA, USA, 2021.
24. Straubinger, A.; Rothfeld, R.; Shamiyeh, M.; Büchter, K.D.; Kaiser, J.; Plötner, K.O. An overview of current research and developments in urban air mobility-Setting the scene for UAM introduction. *J. Air Transp. Manag.* **2020**, *87*, 101852. [CrossRef]
25. Akash, A.; Raj, V.S.J.; Sushmitha, R.; Prateek, B.; Aditya, S.; Sreehari, V.M. Design and Analysis of VTOL Operated Intercity Electrical Vehicle for Urban Air Mobility. *Electronics* **2021**, *11*, 20. [CrossRef]
26. Brunelli, M.; Ditta, C.C.; Postorino, M.N. New infrastructures for urban air mobility systems: A systematic review on vertiport location and capacity. *J. Air Transp. Manag.* **2023**, *112*, 102460. [CrossRef]
27. Schweiger, K.; Preis, L. Urban Air Mobility: Systematic Review of Scientific Publications and Regulations for Vertiport Design and Operations. *Drones* **2022**, *6*, 179. [CrossRef]

28. Chriki, A.; Touati, H.; Snoussi, H.; Kamoun, F. FANET: Communication, mobility models and security issues. *Comput. Netw.* **2019**, *163*, 106877. [CrossRef]
29. Jawhar, I.; Mohamed, N.; Al-Jaroodi, J. UAV-based data communication in wireless sensor networks: Models and strategies. In Proceedings of the 2015 International Conference on Unmanned Aircraft Systems (ICUAS), Denver, CO, USA, 9–12 June 2015; pp. 687–694.
30. Ho, D.T.; Shimamoto, S. Highly reliable communication protocol for WSN-UAV system employing TDMA and PFS scheme. In Proceedings of the 2011 IEEE GLOBECOM Workshops (GC Wkshps), Houston, TX, USA, 5–9 December 2011; pp. 1320–1324.
31. Wang, X.; Yadav, V.; Balakrishnan, S.N. Cooperative UAV formation flying with obstacle/collision avoidance. *IEEE Trans. Control Syst. Technol.* **2007**, *15*, 672–679. [CrossRef]
32. Lee, J.; Park, B. Development and evaluation of a cooperative vehicle intersection control algorithm under the connected vehicles environment. *IEEE Trans. Intell. Transp. Syst.* **2012**, *13*, 81–90. [CrossRef]
33. Demba, A.; Möller, D.P. Vehicle-to-vehicle communication technology. In Proceedings of the 2018 IEEE International Conference on Electro/Information Technology (EIT), Rochester, MI, USA, 3–5 May 2018; pp. 0459–0464.
34. Djahel, S.; Jabeur, N.; Barrett, R.; Murphy, J. Toward V2I communication technology-based solution for reducing road traffic congestion in smart cities. In Proceedings of the 2015 International Symposium on Networks, Computers and Communications (ISNCC), Yasmine Hammamet, Tunisia, 13–15 May 2015; pp. 1–6.
35. Prevot, T.; Rios, J.; Kopardekar, P.; Robinson, J.E., III; Johnson, M.; Jung, J. UAS traffic management (UTM) concept of operations to safely enable low altitude flight operations. In Proceedings of the 16th AIAA Aviation Technology, Integration, and Operations Conference, Washington, DC, USA, 13–17 June 2016; p. 3292.
36. SESAR. U-Space Blueprint. 2017. Available online: https://www.sesarju.eu/sites/default/files/documents/reports/U-space%20Blueprint%20brochure%20final.PDF (accessed on 1 October 2022).
37. Yang, X.; Wei, P. Scalable multi-agent computational guidance with separation assurance for autonomous urban air mobility. *J. Guid. Control. Dyn.* **2020**, *43*, 1473–1486. [CrossRef]
38. Ditta, C.C.; Postorino, M.N. New Challenges for Urban Air Mobility Systems: Aerial Cooperative Vehicles. In Proceedings of the International Symposium on Intelligent and Distributed Computing XIV, Bremen, Germany, 14–16 September 2022; Studies in Computational Intelligence. Springer: Cham, Switzerland, 2022; Volume 1026, pp. 135–145.
39. Samir Labib, N.; Danoy, G.; Musial, J.; Brust, M.R.; Bouvry, P. Internet of unmanned aerial vehicles—A multilayer low-altitude airspace model for distributed UAV traffic management. *Sensors* **2019**, *19*, 4779. [CrossRef]
40. Schalk, L.M.; Peinecke, N. Detect and avoid for unmanned aircraft in very low level airspace. In *Automated Low-Altitude Air Delivery: Towards Autonomous Cargo Transportation with Drones*; Springer: Cham, Switzerland, 2022; pp. 333–351.
41. Xu, C.; Liao, X.; Tan, J.; Ye, H.; Lu, H. Recent research progress of unmanned aerial vehicle regulation policies and technologies in urban low altitude. *IEEE Access* **2020**, *8*, 74175–74194. [CrossRef]
42. Sunil, E.; Hoekstra, J.M.; Ellerbroek, J.; Bussink, F.; Nieuwenhuisen, D.; Vidosavljevic, A.; Kern, S. Metropolis: Relating airspace structure and capacity for extreme traffic densities. In Proceedings of the 11th USA/Europe Air Traffic Management Research and Development Seminar (ATM2015), Lisbon, Portugal, 23–26 June 2015; FAA/Eurocontrol: Washington, DC, USA, 2015.
43. He, Z.; Zhang, B.; Wang, J.; Wang, L.; Ren, Y.; Han, Z. Performance analysis and optimization for V2V-assisted UAV communications in vehicular networks. In Proceedings of the ICC 2020–2020 IEEE International Conference on Communications (ICC), Dublin, Ireland, 7–11 June 2020; pp. 1–6.
44. Pang, B.; Dai, W.; Ra, T.; Low, K.H. A concept of airspace configuration and operational rules for UAS in current airspace. In Proceedings of the 2020 AIAA/IEEE 39th Digital Avionics Systems Conference (DASC), San Antonio, TX, USA, 11–15 October 2020; pp. 1–9.
45. Lascara, B.; Lacher, A.; DeGarmo, M.; Maroney, D.; Niles, R.; Vempati, L. *Urban Air Mobility Airspace Integration Concepts: Operational Concepts and Exploration Approachs*; The MITRE Corporation: Mclean, VA, USA, 2019.
46. Wang, Z.; Delahaye, D.; Farges, J.L.; Alam, S. Complexity optimal air traffic assignment in multi-layer transport network for Urban Air Mobility operations. *Transp. Res. Part C Emerg. Technol.* **2022**, *142*, 103776. [CrossRef]
47. Causa, F.; Franzone, A.; Fasano, G. Strategic and tactical path planning for urban air mobility: Overview and application to real-world use cases. *Drones* **2022**, *7*, 11. [CrossRef]
48. Safadi, Y.; Fu, R.; Quan, Q.; Haddad, J. Macroscopic fundamental diagrams for low-altitude air city transport. *Transp. Res. Part C Emerg. Technol.* **2023**, *152*, 104141. [CrossRef]
49. Tang, H.; Zhang, Y.; Post, J. Predeparture Flight Planning to Minimize Operating Cost for Urban Air Mobility. *J. Air Transp.* **2023**, 1–11. [CrossRef]
50. Brunelli, M.; Ditta, C.C.; Postorino, M.N. A Framework to Develop Urban Aerial Networks by Using a Digital Twin Approach. *Drones* **2022**, *6*, 387. [CrossRef]
51. Chand, B.N.; Mahalakshmi, P.; Naidu, V.P.S. Sense and avoid technology in unmanned aerial vehicles: A review. In Proceedings of the 2017 International Conference on Electrical, Electronics, Communication, Computer, and Optimization Techniques (ICEECCOT), Mysuru, India, 15–16 December 2017; pp. 512–517.
52. Antcliff, K.R.; Moore, M.D.; Goodrich, K.H. Silicon Valley as an early adopter for on-demand civil VTOL operations. In Proceedings of the 16th AIAA Aviation Technology, Integration, and Operations Conference, Washington, DC, USA, 13–17 June 2016; p. 3466.

53. Wu, Z.; Zhang, Y. Optimal eVTOL charging and passenger serving scheduling for on-demand urban air mobility. In Proceedings of the AIAA Aviation 2020 Forum, Virtual Event, 15–19 June 2020; p. 3253.
54. Healy, R.; Misiorwoski, M.; Gandhi, F. A systematic CFD-based examination of rotor-rotor separation effects on interactional aerodynamics for large eVTOL aircraft. In Proceedings of the 75th Vertical Flight Society Annual Forum, Philadelphia, PA, USA, 13–16 May 2019; Volume 2, p. 4.
55. Dijkstra, E.W. A note on two problems in connexion with graphs. *Numer. Math.* **1959**, *1*, 269–271. [CrossRef]
56. Fu, L.; Sun, D.; Rilett, L.R. Heuristic shortest path algorithms for transportation applications: State of the art. *Comput. Oper. Res.* **2006**, *33*, 3324–3343. [CrossRef]
57. Beyne, E.E.; Castro, S.G. Preliminary performance assessment of a long-range eVTOL aircraft. In Proceedings of the AIAA SCITECH 2022 Forum, San Diego, CA, USA, 3–7 January 2022; p. 1030.
58. Ditta, C.C.; Postorino, M.N. A 3D Urban Aerial Network for New Mobility Solutions. In *International Symposium on Intelligent and Distributed Computing XV. Studies in Computational Intelligence*; Springer International Publishing: Cham, Switzerland, 2023; Volume 1089, pp. 277–286.
59. CityAirbus NextGen (Airbus). Available online: https://www.airbus.com/en/innovation/low-carbon-aviation/urban-air-mobility/cityairbus-nextgen (accessed on 1 June 2023).
60. Khayat, G.; Mavromoustakis, C.X.; Mastorakis, G.; Batalla, J.M.; Pallis, E.; Markakis, E.K. Transfer Time Calculation in FANET and WSN Networks in Crisis Scenario. In Proceedings of the 2021 IEEE Global Communications Conference (GLOBECOM), Madrid, Spain, 7–11 December 2021; pp. 1–6.
61. Ma, T.; Wang, X.; Qiao, N.; Zhang, Z.; Fu, J.; Bao, M. A Conceptual Design and Optimization Approach for Distributed Electric Propulsion eVTOL Aircraft Based on Ducted-Fan Wing Unit. *Aerospace* **2022**, *9*, 690. [CrossRef]
62. André, N.; Hajek, M. Robust environmental life cycle assessment of electric VTOL concepts for urban air mobility. In Proceedings of the AIAA Aviation 2019 Forum, Dallas, TX, USA, 17–21 June 2019; p. 3473.
63. Italian Institute for Environmental Protection and Research (ISPRA). *Efficiency and Decarbonisation Indicators in Italy and in the Biggest European Countries*; Edition 2023, Reports 386/2023; ISPRA: Roma, Italy, 2023.
64. Italian Institute for Environmental Protection and Research, ISPRA National Database. Available online: https://fetransp.isprambiente.it/ (accessed on 1 July 2023).
65. COPERT EU Software. Available online: https://www.emisia.com/utilities/copert/versions/ (accessed on 1 July 2023).
66. Mudumba, S.V.; Chao, H.; Maheshwari, A.; DeLaurentis, D.A.; Crossley, W.A. Modeling CO_2 emissions from trips using urban air mobility and emerging automobile technologies. *Transp. Res. Rec.* **2021**, *2675*, 1224–1237. [CrossRef]
67. Kasliwal, A.; Furbush, N.J.; Gawron, J.H.; McBride, J.R.; Wallington, T.J.; De Kleine, R.D.; Kim, H.C.; Keoleian, G.A. Role of flying cars in sustainable mobility. *Nat. Commun.* **2019**, *10*, 1555. [CrossRef]
68. International Standard Atmosphere. Wiley, 2013. Available online: https://onlinelibrary.wiley.com/doi/pdf/10.1002/9781118568101.app2 (accessed on 1 July 2023).
69. News European Parliament: CO2 Emissions from Cars: Facts and Figures (Infographics). Available online: https://www.europarl.europa.eu/news/en/headlines/society/20190313STO31218/co2-emissions-from-cars-facts-and-figures-infographics (accessed on 1 July 2023).
70. Velaz-Acera, N.; Álvarez-García, J.; Borge-Diez, D. Economic and emission reduction benefits of the implementation of eVTOL aircraft with bi-directional flow as storage systems in islands and case study for Canary Islands. *Appl. Energy* **2023**, *331*, 120409. [CrossRef]
71. Coykendal, J.; Metcalfe, M.; Hussain, A.; Dronamraju, T. *Advanced Air Mobility: Disrupting the Future of Mobility*; Deloitte Papers; Deloitte Development LLC: New York, NY, USA, 2022.
72. Zhao, P.; Post, J.; Wu, Z.; Du, W.; Zhang, Y. Environmental impact analysis of on-demand urban air mobility: A case study of the Tampa Bay Area. *Transp. Res. Part D Transp. Environ.* **2022**, *110*, 103438. [CrossRef]
73. Fadhil, D.N. A GIS-Based Analysis for Selecting Ground Infrastructure Locations for Urban Air Mobility. Master's Thesis, Technical University of Munich, Munich, Germany, 2018.
74. Delgado Gonzalez, C.J. Rooftop-Place Suitability Analysis for Urban Air Mobility Hubs: A GIS and Neural Network Approach. Master's Thesis, Universida de Nova de Lisboa, Lisbon, Portugal, 2020.
75. Jeong, J.; So, M.; Hwang, H.Y. Selection of Vertiports Using K-Means Algorithm and Noise Analyses for Urban Air Mobility (UAM) in the Seoul Metropolitan Area. *Appl. Sci.* **2021**, *11*, 5729. [CrossRef]
76. Chen, L.; Wandelt, S.; Dai, W.; Sun, X. Scalable vertiport hub location selection for air taxi operations in a metropolitan region. *INFORMS J. Comput.* **2021**, *34*, 834–856. [CrossRef]
77. Rath, S.; Chow JY, J. Air taxi skyport location problem with single-allocation choice-constrained elastic demand for airport access. *arXiv* **2021**, arXiv:1904.01497v4. [CrossRef]